Analysis of emissivity and absorptivity of two overlapping guided modes in two-dimensional periodic structures

Asano, Takashi; Inoue, Takuya; De Zoysa, Menaka; Noda, Susumu

PHYSICAL REVIEW A **89**, 033811 (2014)

Analysis of emissivity and absorptivity of two overlapping guided modes in two-dimensional periodic structures

Takashi Asano,* Takuya Inoue, Menaka De Zoysa, and Susumu Noda
Department of Electronic Science and Engineering, Kyoto University, Kyoto 615-8510, Japan
(Received 12 October 2013; revised manuscript received 14 December 2013; published 7 March 2014)

The thermal emission from two guided modes in two-dimensional periodic structures is investigated using first-principles calculations. We use a model that integrates a quantum mechanical analysis of light-matter interactions and a classical connection condition that describes the coupling between light modes inside and outside the structure. We focus on what happens when two guided modes share common radiation modes where their thermal emission overlaps in frequency, solid angle, and polarization in free space. It is shown that we have to take into account the fact that the reaction of the radiation from one guided mode works not only on that guided mode but also on the other guided mode, in order to calculate the emissivity from two overlapping guided modes accurately. Emissivity spectra peculiar to the two-guided mode cases are shown. The condition to maximize the light-matter interaction with respect to thermal emission in the case with two guided modes is also discussed.

DOI: 10.1103/PhysRevA.89.033811 PACS number(s): 42.72.Ai, 44.40.+a, 42.70.Qs

I. INTRODUCTION

Thermal emission-control devices [1–15], in which the frequency range, solid angle, and polarization of the radiation are tailored according to specific needs, show promise both as efficient light sources for sensing and illumination, and also as emitters for the (solar) thermophotovoltaic generation of electricity [16,17]. So far, it has been considered that the best method to control thermal radiation is to modify the photonic modes inside a device. The main aim is to control the interaction between light and the material inside which it propagates, as well as to control the connecting condition that describes coupling between light inside and outside the material. Controlled thermal emission has been realized using arrays of metallic cavities and meta-atoms, surface plasmon or polariton modes that are coupled out by periodic structures, and metallic or free-carrier doped photonic crystals [1–10]. In addition, we have previously proposed a method to tune both the electronic and photonic modes inside a device [11], and have recently demonstrated that it enables more efficient control of thermal emission together with a significant increase in power utilization efficiency [13]. It is important to note that these techniques can also be utilized in reverse fashion to control or enhance the absorption spectrum of a material in order to improve the performance of devices such as detectors and photovoltaic cells [18–21].

Thus far, one of the guidelines for designing a thermal emission-control device has been to match the absorption Q value (Q_{abs}) of a photonic mode inside a device with the radiation Q value (Q_{rad}) [9,11]. We note that in the case of a metamaterial field, the concept of impedance matching has also been utilized [12]. Although the Q matching condition maximizes the peak emissivity from a single, isolated photonic mode, in practice multiple modes can exist inside a device. It is expected that utilization of multiple photonic modes would increase the controllability and enhancement of emission and absorption. However, the consequences of overlap between emissions from these multiple modes are still unclear. In this paper, we discuss the effect theoretically using a model based on planar thermal emission-control devices, where the optical modes concerned can be treated as two-dimensional (2D) guided modes. We discuss the situation where two guided modes share common radiation modes and their thermal emission overlaps in frequency, solid angle, and polarization in free space. In such a situation, simple application of the Q matching condition to the two guided modes might lead to emissivity greater than unity in the region of overlap. However, our analysis indicates that the emissivity does not exceed unity, when the interaction between the two guided modes via common radiation modes is taken into account correctly. We also investigate how strongly the light-matter interaction can be controlled or enhanced in the two-guided-modes case compared to one-resonant-mode case as concerned with emissivity and absorptivity spectra. Our results supply a physical understanding of multimode thermal emission, and also contribute to a development of methods to control the emissivity and absorptivity spectrum according to specific requirements.

II. THEORY

Figure 1 shows the schematic model used for our analysis, where a 2D guided mode interacts with a thermal bath of temperature T_{TB} and with free-space modes of temperature T_{FS}. For simplicity we assume that a periodic square lattice couples guided modes with free-space modes and that no emission to the lower half of the structure ($z < 0$) occurs. The lattice constant and dimensions of the device are defined as a and $L \times L$, respectively, and the size of free space is defined as $L^2 L_z$. We discuss the situation where two guided modes exist, which overlap with respect to frequency and solid angle region (and polarization), as shown in Fig. 2. In this case, components of the two guided modes with the same in-plane wave vector $\vec{k}_{//}$ can interfere. Figure 3 shows the model used for our analysis. Components of each guided mode, both with the same $\vec{k}_{//}$, are picked up and modeled as two photonic modes represented by the annihilation operators $\hat{a}_1$ and $\hat{a}_2$. They couple to radiation modes represented by $\hat{d}_\mu$ that have the same $\vec{k}_{//}$. Each guided mode is assumed to couple to two

*tasano@qoe.kuee.kyoto-u.ac.jp

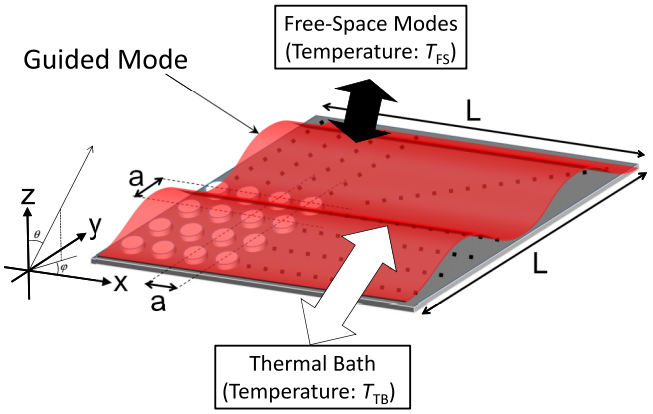

FIG. 1. (Color online) Schematic illustration of the model used for theoretical analysis of thermal emission, where a guided mode in a 2D periodic structure interacts with a thermal bath of temperature T_{TB} and free-space modes of temperature T_{FS}. Different 2D guided modes are assumed to interact with different independent thermal baths and common free-space modes (see also Figs. 2 and 3).

independent bosonic thermal baths represented by $\hat{b}_{1\mu}$ and $\hat{b}_{2\mu}$ (see Appendix A for the details).

The Hamiltonian of this model is given by

$$\hat{H} = \hbar\omega_{a1}\hat{a}_1^\dagger\hat{a}_1 + \hbar\omega_{a2}\hat{a}_2^\dagger\hat{a}_2 + \sum_\mu \hbar\omega_{d\mu}\hat{d}_\mu^\dagger\hat{d}_\mu + \sum_\mu \hbar\omega_{b1\mu}\hat{b}_{1\mu}^\dagger\hat{b}_{1\mu} + \sum_\mu \hbar\omega_{b2\mu}\hat{b}_{2\mu}^\dagger\hat{b}_{2\mu}$$

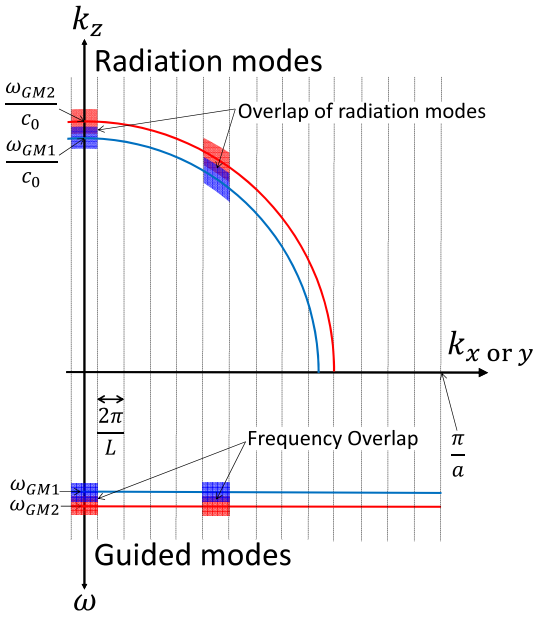

FIG. 2. (Color online) Schematic illustration showing the case where two 2D guided modes overlap in frequency. The lower part shows dispersion curves of the two 2D guided modes and the upper part shows wave-vector–space distribution of the radiation modes that couple to the two 2D guided modes where the frequency of the modes are projected onto k_z. The overlap of thermal radiation modes can occur for the 2D guided modes with the same in-plane wave vectors and with spectral overlaps.

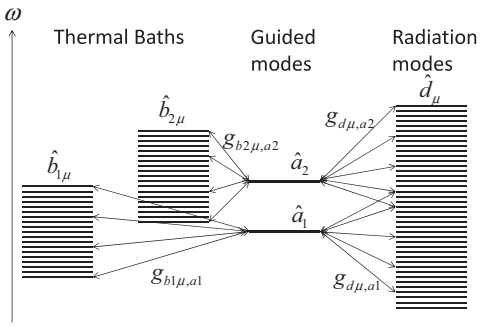

FIG. 3. Model used for the analysis consisting of a pair of guided modes, two independent thermal baths, and a set of common radiation modes. Both guided modes are assumed to interact with different independent thermal baths but radiation modes are common and possible to overlap (see also Fig. 2).

$$+\hbar\sum_\mu (g_{d\mu,a1}\hat{d}_\mu\hat{a}_1^\dagger + g_{d\mu,a1}^*\hat{d}_\mu^\dagger\hat{a}_1) + \hbar\sum_\mu (g_{d\mu,a2}\hat{d}_\mu\hat{a}_2^\dagger + g_{d\mu,a2}^*\hat{d}_\mu^\dagger\hat{a}_2) + \hbar\sum_\mu (g_{b1\mu,a1}\hat{b}_{1\mu}\hat{a}_1^\dagger + g_{b1\mu,a1}^*\hat{b}_{1\mu}^\dagger\hat{a}_1) + \hbar\sum_\mu (g_{b2\mu,a2}\hat{b}_{2\mu}\hat{a}_2^\dagger + g_{b2\mu,a1}^*\hat{b}_{2\mu}^\dagger\hat{a}_2), \quad (1)$$

where ω_α is the frequency of mode α, and $g_{\alpha,\beta}$ is the coupling constant between modes α and β. By formally integrating the Heisenberg equation of motion for $\hat{d}_\mu$ under the first-order approximation that the main frequency component of $\hat{a}_1(t)$ is ω_{a1}, we can obtain an expression for $\hat{d}_\mu$ as follows:

$$\hat{d}_\mu(t) = \hat{d}_\mu(t_0)\exp[-i\omega_{d\mu}(t-t_0)] - ig_{d\mu,c1}^*\hat{a}_1(t)\int_{t0}^{t}\exp[-i(\omega_{d\mu}-\omega_{a1})(t-\tau)]d\tau - ig_{d\mu,a2}^*\hat{a}_2(t)\int_{t0}^{t}\exp[-i(\omega_{d\mu}-\omega_{a2})(t-\tau)]d\tau. \quad (2)$$

An expression for $\hat{b}_{1\mu}$ can be obtained by the same method. Substituting into the Heisenberg equation of motion for $\hat{a}_1$ gives the following:

$$\frac{d\hat{a}_1(t)}{dt} = -i\omega_{a1}\hat{a}_1(t) - i\sum_\mu g_{d\mu,a1}\hat{d}_\mu(t_0)\exp[-i\omega_{d\mu}(t-t_0)] - \hat{a}_1(t)\sum_\mu |g_{d\mu,a1}|^2\pi\delta(\omega_{d\mu}-\omega_{a1}) - \hat{a}_2(t)\sum_\mu g_{d\mu,a1}g_{d\mu,a2}^*\pi\delta(\omega_{d\mu}-\omega_{a2}) - i\sum_\mu g_{b1\mu,a1}\hat{b}_{1\mu}(t_0)\exp[-i\omega_{b1\mu}(t-t_0)] - \hat{a}_1(t)\sum_\mu |g_{b1\mu,a1}|^2\pi\delta(\omega_{b1\mu}-\omega_{a1}), \quad (3)$$

where the fourth term on the right represents the reaction from the radiation modes excited by $\hat{a}_2$, which can be also understood as the coupling between the two guided modes via common radiation modes. Following the same method, the equation of motion for $\hat{a}_2$ is also obtained. We define the noise terms and decay and mutual coupling constants as follows:

$$-i\sum_{\mu}\hat{\alpha}_{\mu}(t_0)g_{\alpha\mu,ai}\exp[-i\omega_{\alpha\mu}(t-t_0)] \equiv \hat{f}_{\alpha,i}(t), \quad (4)$$

$$\sum_{\mu} g_{\alpha\mu,ai}g^{*}_{\alpha\mu,aj}\pi\delta(\omega_{\alpha\mu}-\omega_{aj}) = \pi D_{\alpha}(\omega_{aj})\overline{g_{\alpha,ai}g^{*}_{\alpha,aj}(\omega_{aj})} \equiv \gamma_{\alpha,ij}. \quad (5)$$

Here $\hat{\alpha}_{\mu}$ is $\hat{d}_{\mu}$ or $\hat{b}_{1\mu}$ or $\hat{b}_{2\mu}$, $D_{\alpha}(\omega)$ is the density of states of modes $\hat{\alpha}_{\mu}$, and subscripts i, j identify the cavity modes (1 or 2). The term $\gamma_{\alpha,ij}$ does not exist for $i \neq j$ when $\hat{\alpha}_{\mu} = \hat{b}_1$ or $\hat{b}_2$ because the two thermal baths are independent. Using these definitions, Eq. (3) and its counterpart can be written together in the form of a system of equations as follows:

$$\frac{d}{dt}\begin{pmatrix}\hat{a}_1(t)\\ \hat{a}_2(t)\end{pmatrix} = \begin{pmatrix}\hat{f}_{d,1}(t)\\ \hat{f}_{d,2}(t)\end{pmatrix} + \begin{pmatrix}\hat{f}_{b1,1}(t)\\ \hat{f}_{b2,2}(t)\end{pmatrix} + Q\begin{pmatrix}\hat{a}_1(t)\\ \hat{a}_2(t)\end{pmatrix}, \quad (6)$$

where Q is the characteristic matrix of this system given by

$$Q = \begin{pmatrix}-i\omega_{a1}-\gamma_{d,11}-\gamma_{b1,11} & -\gamma_{d,12}\\ -\gamma_{d,21} & -i\omega_{a2}-\gamma_{d,22}-\gamma_{b2,22}\end{pmatrix}. \quad (7)$$

We define the eigenvalues of Q as λ_+ and λ_- and the corresponding eigenvectors as $\vec{p}_+$ and $\vec{p}_-$, respectively. By using a matrix composed of the two (column) eigenvectors $P = (\vec{p}_+, \vec{p}_-)$, Q can be diagonalized as $P^{-1}QP = \begin{pmatrix}\lambda_+ & 0\\ 0 & \lambda_-\end{pmatrix} = \Lambda$ when the eigenvalues are nondegenerate. Applying this diagonalization to Eq. (6), we obtain

$$\frac{d}{dt}\begin{pmatrix}\hat{a}_+(t)\\ \hat{a}_-(t)\end{pmatrix} = P^{-1}\begin{pmatrix}\hat{f}_{d,1}(t)\\ \hat{f}_{d,2}(t)\end{pmatrix} + P^{-1}\begin{pmatrix}\hat{f}_{b1,1}(t)\\ \hat{f}_{b2,2}(t)\end{pmatrix} + \Lambda\begin{pmatrix}\hat{a}_+(t)\\ \hat{a}_-(t)\end{pmatrix}, \quad (8)$$

where $\begin{pmatrix}\hat{a}_+(t)\\ \hat{a}_-(t)\end{pmatrix} = P^{-1}\begin{pmatrix}\hat{a}_1(t)\\ \hat{a}_2(t)\end{pmatrix}$ represents reconfigured eigenmodes of which frequency and decay constants are represented by λ_+ and λ_-, respectively.

In the following, we ignore the noise terms of the free-space modes because the temperature T_{FS} is assumed to be much lower than that of the thermal baths (T_{TB}). By formally integrating (8), substituting it into the Heisenberg equation of motion for $\hat{d}_{\mu}$, and formally integrating again, we obtain

$$\hat{d}_{\mu}(t) = -i(g^{*}_{d\mu,a+}, g^{*}_{d\mu,a-})\int_{t_0}^{t}d\tau\int_{t_0}^{\tau}d\tau' \times \exp[\Lambda(\tau-\tau')]P^{-1}\begin{pmatrix}\hat{f}_{b1,1}(\tau')\\ \hat{f}_{b2,2}(\tau')\end{pmatrix} \times \exp[-i\omega_{d\mu}(t-\tau)] \quad (9)$$

for t sufficiently larger than the inverse of the decay constants, where we defined the coupling constants for reconfigured eigenmodes $\hat{a}_+$,$\hat{a}_-$ as $(g^{*}_{d\mu,a+}, g^{*}_{d\mu,a-}) = (g^{*}_{\mu,a1}, g^{*}_{\mu,a2})P$. The radiation power spectrum to free space $P_{em}(\omega)$ is obtained by Fourier transformation of the rate of increase of the total energy of the free-space modes (see Appendix B for the details) as follows:

$$P_{em}(\omega) = \frac{\hbar\omega}{2\pi}\int_{-\infty}^{+\infty}\sum_{\mu}\frac{d}{dt}\langle\hat{d}^{\dagger}_{\mu}(t+\tau)\hat{d}_{\mu}(t)\rangle\exp(-i\omega\tau)d\tau. \quad (10)$$

From (9) we obtain

$$\hat{d}^{\dagger}_{\mu}(t)\hat{d}_{\mu}(t') = \int_0^t d\tau\int_0^{\tau}d\tau'\int_0^{t'}d\tau''\int_0^{\tau''}d\tau'''(g_{d\mu,a+}, g_{d\mu,a-})\exp[\Lambda^{*}(\tau-\tau')]P^{-1*}\begin{pmatrix}\hat{f}^{\dagger}_{b1,1}(\tau')\\ \hat{f}^{\dagger}_{b2,2}(\tau')\end{pmatrix}(\hat{f}^{\dagger}_{b1,1}(\tau'''), \hat{f}^{\dagger}_{b2,2}(\tau'''))P^{-1T} \times \exp[\Lambda(\tau''-\tau''')]\begin{pmatrix}g^{*}_{d\mu,a+}\\ g^{*}_{d\mu,a-}\end{pmatrix}\exp[+i\omega_{d\mu}(t-\tau)]\exp[-i\omega_{d\mu}(t'-\tau'')]. \quad (11)$$

The expectation value of the correlation term in Eq. (11) can be calculated as follows:

$$\left\langle\begin{pmatrix}\hat{f}^{\dagger}_{b1,1}(\tau')\\ \hat{f}^{\dagger}_{b2,2}(\tau')\end{pmatrix}(\hat{f}_{b1,1}(\tau'''), \hat{f}_{b2,2}(\tau'''))\right\rangle = \sum_{\mu'}\exp[i\omega_{b\mu'}(\tau'-\tau''')]\bar{n}_{\mathrm{res}}(\omega_{b\mu'})\begin{pmatrix}|g_{b1\mu',a1}|^2 & 0\\ 0 & |g_{b2\mu',a2}|^2\end{pmatrix}, \quad (12)$$

where $\bar{n}_{\mathrm{res}}(\omega) = \{\exp(\hbar\omega/k_{\mathrm{B}}T_{TB}) - 1\}^{-1}$, and we renamed the notation for the frequency of two thermal bath modes $\omega_{b1\mu'} = \omega_{b2\mu'} \equiv \omega_{b\mu'}$. By substituting (12) into (11) and using the relation $(a,b)\begin{pmatrix}c & 0\\ 0 & d\end{pmatrix} = (c,d)\begin{pmatrix}a & 0\\ 0 & b\end{pmatrix}$, we obtain

$$\langle\hat{d}^{\dagger}_{\mu}(t)\hat{d}_{\mu}(t')\rangle = \int_0^t d\tau\int_0^{\tau}d\tau'\int_0^{t'}d\tau''\int_0^{\tau''}d\tau'''\sum_{\mu'}n_{\mathrm{res}}(\omega_{b\mu'})\exp[+i\omega_{d\mu}(t-\tau)]\exp[-i\omega_{d\mu}(t'-\tau'')]\exp[i\omega_{b\mu'}(\tau'-\tau''')] \times \mathrm{Tr}\left[\begin{pmatrix}\exp[\lambda^{*}_{+}(\tau-\tau')]\exp[\lambda_{+}(\tau''-\tau''')] & \exp[\lambda^{*}_{+}(\tau-\tau')]\exp[\lambda_{-}(\tau''-\tau''')]\\ \exp[\lambda^{*}_{-}(\tau-\tau')]\exp[\lambda_{+}(\tau''-\tau''')] & \exp[\lambda^{*}_{-}(\tau-\tau')]\exp[\lambda_{-}(\tau''-\tau''')]\end{pmatrix}\Theta\right], \quad (13)$$

where time-independent 2×2 matrix Θ is given as follows:

$$\Theta = \begin{pmatrix} g_{d\mu,a+} & 0 \\ 0 & g_{d\mu,a-} \end{pmatrix} P^{-1*} \begin{pmatrix} |g_{b1\mu',a1}|^2 & 0 \\ 0 & |g_{b2\mu',a2}|^2 \end{pmatrix} P^{-1T} \begin{pmatrix} g^*_{d\mu,a+} & 0 \\ 0 & g^*_{d\mu,a-} \end{pmatrix}. \tag{14}$$

We note that the time-dependent term of Eq. (13) can be calculated as follows:

$$\begin{aligned} F(t,t') &= \int_0^t d\tau \int_0^\tau d\tau' \int_0^{t'} d\tau'' \int_0^{\tau''} d\tau''' \exp[+i\omega_{d\mu}(t-\tau)] \exp[-i\omega_{d\mu}(t'-\tau'')] \exp[i\omega_{b\mu'}(\tau'-\tau''')] \\ &\quad \times \begin{pmatrix} \exp[\lambda^*_+(\tau-\tau')] \exp[\lambda_+(\tau''-\tau''')] & \exp[\lambda^*_+(\tau-\tau')] \exp[\lambda_-(\tau''-\tau''')] \\ \exp[\lambda^*_-(\tau-\tau')] \exp[\lambda_+(\tau''-\tau''')] & \exp[\lambda^*_-(\tau-\tau')] \exp[\lambda_-(\tau''-\tau''')] \end{pmatrix} \\ &\approx 2\pi\delta(\omega_{b\mu'}-\omega_{d\mu})t' \exp[+i\omega_{d\mu}(t-t')] \begin{pmatrix} \frac{1}{(\lambda_++i\omega_{d\mu})(\lambda^*_+-i\omega_{d\mu})} & \frac{1}{(\lambda_-+i\omega_{d\mu})(\lambda^*_+-i\omega_{d\mu})} \\ \frac{1}{(\lambda_++i\omega_{d\mu})(\Lambda^*_--i\omega_{d\mu})} & \frac{1}{(\lambda_-+i\omega_{d\mu})(\lambda^*_--i\omega_{d\mu})} \end{pmatrix}, \end{aligned} \tag{15}$$

for the time t, t' enough larger than the inverse of the decay constants. By substituting Eqs. (13)–(15) into (10), we obtain

$$P_{em}(\omega) = \frac{2}{\pi}\bar{n}_{\rm res}(\omega)\hbar\omega \mathrm{Tr}\left[\begin{pmatrix} \frac{1}{(\lambda_++i\omega)(\lambda^*_+-i\omega)} & \frac{1}{(\lambda_-+i\omega)(\lambda^*_+-i\omega)} \\ \frac{1}{(\lambda_++i\omega)(\lambda^*_--i\omega)} & \frac{1}{(\lambda_-+i\omega)(\lambda^*_--i\omega)} \end{pmatrix} \Theta' \right], \tag{16}$$

where $\Theta\prime$ is given as follows:

$$\begin{aligned} \Theta' &= \sum_\mu \pi\delta(\omega_{d\mu}-\omega) \begin{pmatrix} g_{d\mu,a+} & 0 \\ 0 & g_{d\mu,a-} \end{pmatrix} P^{-1*} \\ &\quad \times \begin{pmatrix} \sum_{\mu'} \pi\delta(\omega_{b1\mu'}-\omega)|g_{b1\mu',a1}|^2 & 0 \\ 0 & \sum_{\mu'} \pi\delta(\omega_{b2\mu'}-\omega)|g_{b2\mu',a2}|^2 \end{pmatrix} P^{-1T} \begin{pmatrix} g^*_{d\mu,a+} & 0 \\ 0 & g^*_{d\mu,a-} \end{pmatrix}. \end{aligned} \tag{17}$$

For the case where the density of states and the coupling constants have negligible dependence on frequency in the range of the emission spectrum, we can assume that the decay constants can be written by the product of the coupling constants as follows:

$$\gamma_{\alpha,ij} = \kappa_{\alpha,ai}\kappa^*_{\alpha,aj}, \quad \text{with} \quad \kappa_{\alpha,ai} = \sqrt{\pi D_\alpha(\omega_{ai})}\, g_{\alpha,ai}. \tag{18}$$

By using this notation, Eq. (17) can be written as follows:

$$\Theta' = \begin{pmatrix} \kappa_{d,a+} & 0 \\ 0 & \kappa_{d,a-} \end{pmatrix} P^{-1*} \begin{pmatrix} \kappa_{b1,a1}\kappa^*_{b1,1} & 0 \\ 0 & \kappa_{b2,a2}\kappa^*_{b2,2} \end{pmatrix} P^{-1T} \begin{pmatrix} \kappa^*_{d,a+} & 0 \\ 0 & \kappa^*_{d,a-} \end{pmatrix}, \tag{19}$$

where $(\kappa_{d,a+},\kappa_{d,a-}) = (\kappa_{d,a1},\kappa_{d,a2})P^*$. By substituting this into Eq. (16) we obtain

$$P_{em}(\omega) = \frac{2}{\pi}\bar{n}_{\rm res}(\omega)\hbar\omega\vec{s}(\omega)\vec{s}^{T*}(\omega), \tag{20}$$

where

$$\begin{aligned} \vec{s}(\omega) &= \left(\frac{1}{\lambda_+ + i\omega} \frac{1}{\lambda_- + i\omega} \right) \begin{pmatrix} \kappa_{d,a+} & 0 \\ 0 & \kappa_{d,a-} \end{pmatrix} P^{-1*} \begin{pmatrix} \kappa_{b1,a1} & 0 \\ 0 & \kappa_{b2,a2} \end{pmatrix} \\ &= \frac{1}{(\det P)^*} \left(\frac{\kappa_{d,a+}P^*_{22}\kappa_{b1,a1}}{\lambda_+ + i\omega} - \frac{\kappa_{d,a-}P^*_{21}\kappa_{b1,a1}}{\lambda_- + i\omega} - \frac{\kappa_{d,a+}P^*_{12}\kappa_{b2,a2}}{\lambda_+ + i\omega} + \frac{\kappa_{d,a-}P^*_{11}\kappa_{b2,a2}}{\lambda_- + i\omega} \right). \end{aligned} \tag{21}$$

Here, P_{ij} is the element of eigenvector matrix P in the ith row and jth column. More explicitly the power spectrum equation (20) is written as follows:

$$P_{\rm em}(\omega) = \frac{2\hbar\omega\bar{n}_{\rm res}(\omega)}{\pi\,|\det P|^2} \left[\left| \frac{\kappa_{d,a+}P^*_{22}}{\lambda_+ + i\omega} - \frac{\kappa_{d,a-}P^*_{21}}{\lambda_- + i\omega} \right|^2 \gamma_{b1,11} + \left| -\frac{\kappa_{d,a+}P^*_{12}}{\lambda_+ + i\omega} + \frac{\kappa_{d,a-}P^*_{11}}{\lambda_- + i\omega} \right|^2 \gamma_{b2,22} \right]. \tag{22}$$

The first (second) term of Eq. (22) represents the radiation from the two reconfigured eigenmodes $\hat{a}_+$,$\hat{a}_-$ excited by the first (second) thermal bath. Each term thus describes the interference of radiation from the two eigenmodes excited by the same thermal bath. This interference determines the characteristics of emission spectrum for the overlapping region, and will be discussed in detail in the next section. No interference occurs between the first and second terms because the thermal baths are uncorrelated.

Next we discuss the classical connection condition between the emission power spectrum and the emissivity spectrum. An emission power component of the guided modes with frequency $(\omega \pm \Delta\omega/2)$ and $\vec{k}_{//}(k_x \pm \pi/L, k_y \pm \pi/L)$ couples with free-space modes in the wave-vector range $[k_x \pm \pi/L, k_y \pm \pi/L, (\omega \pm \Delta\omega/2)/(c_0 \cos\theta)]$, where $\theta = \sin^{-1}(c_0|\vec{k}_{//}|/\omega)$. The number

of free-space modes in this range is $N_{fs} = \Delta\omega L_z/2\pi \cos\theta$. The radiation power spectrum for these free-space modes $P_{fs}(\omega)$ can be expressed as

$$P_{fs}(\omega) = \frac{\hbar\omega\bar{n}_{fs}}{L^2 L_z} c_0 N_{fs} L^2 \cos\theta \frac{1}{\Delta\omega} = \frac{\hbar\omega\bar{n}_{fs}}{2\pi}, \tag{23}$$

where the average photon number of each mode is assumed to be $\bar{n}_{fs}$. $\hbar\omega\bar{n}_{fs}c_0/L^2L_z$ is the light intensity of the radiation mode and $L^2\cos\theta$ is the apparent area of the emitter. By letting $P_{fs}(\omega) = P_{em}(\omega)$, we can determine $\bar{n}_{fs}$, which results in the relationship

$$\bar{n}_{fs}(\omega) = \frac{2\pi}{\hbar\omega} P_{em}(\omega). \tag{24}$$

Therefore, the radiation intensity I observed is obtained as

$$I(\omega) = \frac{1}{4\pi} D_d(\omega)\hbar\omega\bar{n}_{fs}c_0 = \frac{\omega^2}{4\pi^2 c_0^2} P_{em}(\omega). \tag{25}$$

The emissivity $\varepsilon(\omega)$ is obtained by substituting Eq. (22) into Eq. (25) and dividing it by the single-polarization blackbody radiation intensity $I_{BB} = \hbar\omega^3\bar{n}_{\rm res}(\omega)/8\pi^3 c_0^2$ as follows:

$$\varepsilon(\omega) = \frac{4}{|\det P|^2}\left[\left|\frac{\kappa_{d,a+}P_{22}^*}{\lambda_+ + i\omega} - \frac{\kappa_{d,a-}P_{21}^*}{\lambda_- + i\omega}\right|^2 \gamma_{b1,11} + \left|-\frac{\kappa_{d,a+}P_{12}^*}{\lambda_+ + i\omega} + \frac{\kappa_{d,a-}P_{11}^*}{\lambda_- + i\omega}\right|^2 \gamma_{b2,22}\right]. \tag{26}$$

The absorptivity (the ratio of light power absorbed by an object compared to the light power incident to the object) of this structure is also obtained by Eq. (26) according to the Kirchhoff's law of radiation that states the emissivity is equal to the absorptivity for a given frequency.

III. RESULTS AND DISCUSSIONS

A. Mechanism for thermal radiation from two resonant modes not to exceed unity

The characteristics of Eq. (26) largely depend on the eigenvalues of Q [Eq. (7)], which are expressed as

$$\lambda_\pm = \frac{-i\omega_{a1} - \gamma_{d,11} - \gamma_{b1,11} - i\omega_{a2} - \gamma_{d,22} - \gamma_{b2,22}}{2} \mp \sqrt{B/4}. \tag{27}$$

Here, B is given by

$$B = (-i\omega_{a1} - \gamma_{d,11} - \gamma_{b1,11} + i\omega_{a2} + \gamma_{d,22} + \gamma_{b2,22})^2 + 4|\gamma_{d,12}|^2. \tag{28}$$

The eigenvector matrix P can be written as follows:

$$P = \begin{pmatrix} \gamma_{d,12} & -i\omega_{a2} - \gamma_{d,22} - \gamma_{b1,22} - \lambda_- \\ -i\omega_{a1} - \gamma_{d,11} - \gamma_{b1,11} - \lambda_+ & \gamma_{d,21} \end{pmatrix}. \tag{29}$$

Here, we focus on the case where the original two modes are identical ($\gamma_{d,11} = \gamma_{d,22} = \gamma_{\rm rad}, \gamma_{b1,11} = \gamma_{b2,22} = \gamma_{\rm abs}$) except for the detuning. In this case the eigenvalues are obtained as

$$\lambda_\pm = -i\bar{\omega} - \gamma_{\rm rad} - \gamma_{\rm abs} \mp \sqrt{\gamma_{\rm rad}^2 - (\omega_{a2} - \omega_{a1})^2/4}, \tag{30}$$

where $\bar{\omega} = (\omega_{a1} + \omega_{a2})/2$. Figure 4 shows examples of the emissivity spectra for the identical two modes calculated by using Eq. (26) for various detuning $\omega_{a2} - \omega_{a1}$ and absorption decay constants $\gamma_{\rm abs}$, where $\gamma_{\rm rad}$ is fixed at $0.05\omega_{a1}$ and all the parameters are normalized by ω_{a1}. It is seen in the figure that the peak emissivity does not exceed unity. Analytical demonstration for the emissivity not to exceed unity in the case of two identical modes is given in Appendix C.

In the following, we will discuss the physical mechanism that explains why the emissivity does not exceed unity case by case.

1. *Large detuning case (i): $|\omega_{a2} - \omega_{a1}| \gg 2\gamma_{\rm rad}$*

When the detuning $|\omega_{a2} - \omega_{a1}|$ is much larger than $2\gamma_{\rm rad}$, we obtain $\lambda_\pm \sim -i\omega_{a1} - \gamma_{\rm rad} - \gamma_{\rm abs}, -i\omega_{a2} - \gamma_{\rm rad} - \gamma_{\rm abs}$ from Eq. (30), and the eigenvector matrix is

$$P \sim \begin{pmatrix} \gamma_{d,12} & 0 \\ 0 & \gamma_{d,21} \end{pmatrix}. \tag{31}$$

Therefore, the emissivity spectrum is given as

$$\varepsilon(\omega) \sim 4\left[\left|\frac{\sqrt{\gamma_{\rm rad}}\sqrt{\gamma_{\rm abs}}}{i(\omega - \omega_{a1}) - \gamma_{\rm rad} - \gamma_{\rm abs}}\right|^2 + \left|\frac{\sqrt{\gamma_{\rm rad}}\sqrt{\gamma_{\rm abs}}}{i(\omega - \omega_{a2}) - \gamma_{\rm rad} - \gamma_{\rm abs}}\right|^2\right]. \tag{32}$$

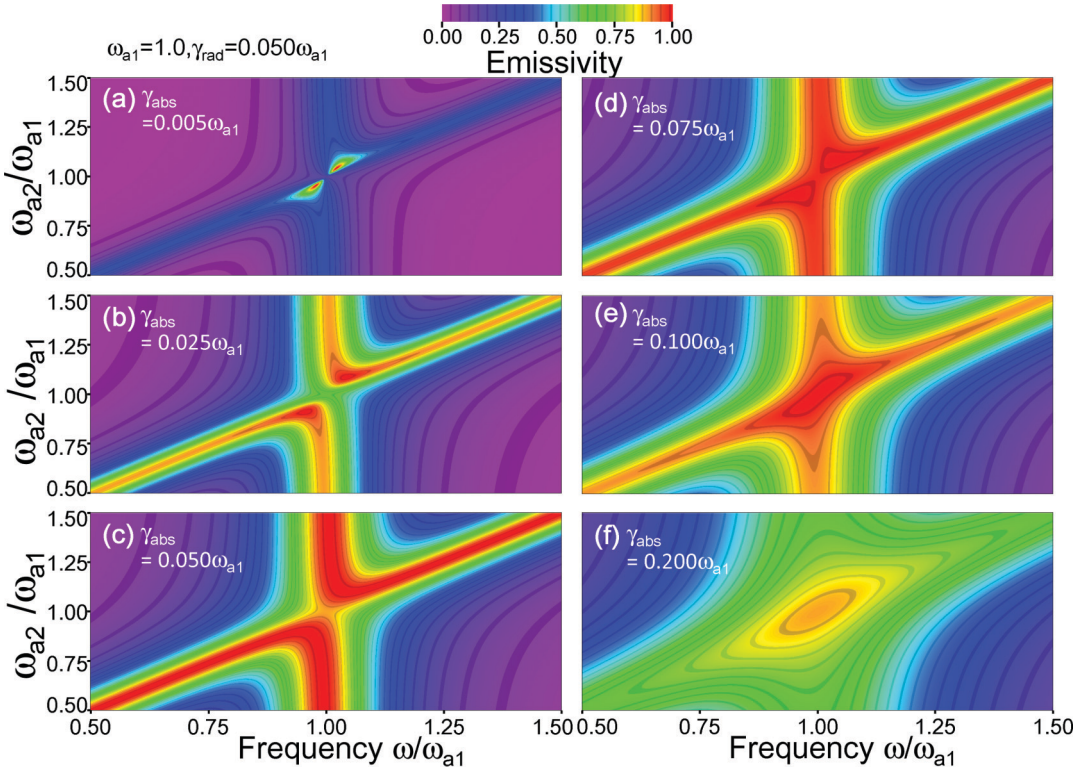

FIG. 4. (Color) Examples of emissivity spectra from two identical cavities for various detunings between ω_{a1} and ω_{a2} and various $\gamma_{\rm abs}(=\gamma_{b1,11}=\gamma_{b2,22})$. All theparameters are normalized byω_{a1}. $\gamma_{\rm rad}(=\gamma_{d,11}=\gamma_{d,22})$ is fixed at $0.05\omega_{a1}$. It is seen that the emissivity is prevented from exceeding unity for all the cases regardless of the spectral overlap.

This means two modes are independent due to the large detuning. Each Lorentzian curve represents the emissivity from each eigenmode. Although the emissivity is summed in the overlapping region, it does not exceed unity due to the large detuning. The peak values at $\omega=\omega_{a1},\omega_{a2}$ approach unity when $\gamma_{\rm rad}\sim\gamma_{\rm abs}$ or matching condition for a single resonant mode is fulfilled. The spectra shown in Fig. 4(c) (where $\gamma_{\rm abs}=0.05\omega_{a1}$ and $\gamma_{\rm rad}=0.05\omega_{a1}$) with $\omega_{a2}\ll 0.9$ or $\omega_{a2}\gg 1.1$ correspond to this case.

2. *Small detuning case (ii):* $|\omega_{a2}-\omega_{a1}|\leqslant 2\gamma_{\rm rad}$

When the detuning is smaller than $2\gamma_{\rm rad}$, the eigenvalues can be written as follows:

$$\lambda_+=-i\bar{\omega}-2\cos^2(\varphi/2)\gamma_{\rm rad}-\gamma_{\rm abs}, \tag{33a}$$

$$\lambda_-=-i\bar{\omega}-2\sin^2(\varphi/2)\gamma_{\rm rad}-\gamma_{\rm abs}, \tag{33b}$$

where

$$\varphi=\tan^{-1}\left(\Delta/\sqrt{\gamma_{\rm rad}^2-\Delta^2}\right)\quad\text{with}\quad\Delta=(\omega_{a2}-\omega_{a1})/2. \tag{34}$$

This means the two eigenmodes have the same frequency and different decay constants. The eigenvector matrix P can be written as follows:

$$P=\gamma_{\rm rad}\begin{pmatrix}e^{i(\theta_1-\theta_2)} & -e^{i\varphi}\\ e^{i\varphi} & e^{-i(\theta_1-\theta_2)}\end{pmatrix}, \tag{35}$$

where $\theta_i=\arg(\kappa_{di})$. By substituting Eqs. (33)–(35) into Eq. (26), the emissivity is obtained as follows:

$$\varepsilon(\omega)=\frac{2}{\cos^2\varphi}\left\{\left|\frac{[\sqrt{2}\cos(\varphi/2)\sqrt{\gamma_{\rm rad}}]\sqrt{\gamma_{\rm abs}}}{i(\bar{\omega}-\omega)-2\cos^2(\varphi/2)\gamma_{\rm rad}-\gamma_{\rm abs}}-\frac{ie^{-i\varphi}[\sqrt{2}\sin(\varphi/2)\sqrt{\gamma_{\rm rad}}]\sqrt{\gamma_{\rm abs}}}{i(\bar{\omega}-\omega)-2\sin^2(\varphi/2)\gamma_{\rm rad}-\gamma_{\rm abs}}\right|^2\right.$$
$$\left.+\left|\frac{[\sqrt{2}\cos(\varphi/2)\sqrt{\gamma_{\rm rad}}]\sqrt{\gamma_{\rm abs}}}{i(\bar{\omega}-\omega)-2\cos^2(\varphi/2)\gamma_{\rm rad}-\gamma_{\rm abs}}+\frac{ie^{+i\varphi}[\sqrt{2}\sin(\varphi/2)\sqrt{\gamma_{\rm rad}}]\sqrt{\gamma_{\rm abs}}}{i(\bar{\omega}-\omega)-2\sin^2(\varphi/2)\gamma_{\rm rad}-\gamma_{\rm abs}}\right|^2\right\}. \tag{36}$$

3. Subcase (ii-a): $\omega_{a2} \sim \omega_{a1}$

When $\varphi \sim 0$ or $\omega_{a2} \sim \omega_{a1}$, the eigenmodes are nearly symmetriclike and antisymmetriclike about the radiation, where the radiation decay constants of $\hat{a}_+(t)$ $(= 2\cos^2(\varphi/2)\gamma_{\rm rad}) \sim 2\gamma_{\rm rad}$ and that of $\hat{a}_-(t)$ $(= 2\sin^2(\varphi/2)\gamma_{\rm rad}) \ll 2\gamma_{\rm rad}$. It is also noted that emission from these two eigenmodes scarcely interferes at $\omega \sim \bar{\omega}$, where the largest overlap occurs, because the radiation from $\hat{a}_+$ and that from $\hat{a}_-$ have a phase difference of $\pi/2$ as can be seen in Eq. (36) with $\varphi \sim 0$. There are two cases to obtain a high-emissivity peak: (a) When $\gamma_{\rm abs} = 2\cos^2(\varphi/2)\gamma_{\rm rad}$ the symmetriclike eigenmode dominates the emission, and the emission from the antisymmetric mode is negligible because of a large mismatch between $2\sin^2(\varphi/2)\gamma_{\rm rad}$ and $\gamma_{\rm abs}[= 2\cos^2(\varphi/2)\gamma_{\rm rad}]$. (b) In contrast, when $\gamma_{\rm abs} = 2\sin^2(\varphi/2)\gamma_{\rm rad}$, antisymmetriclike eigenmode dominates the emission due to the same reason. The emissivity is prevented from exceeding unity because the matching conditions for $\hat{a}_+$ and $\hat{a}_-$ are largely different, and therefore the emission from both eigenmodes cannot simultaneously approach unity.

The examples corresponding to the above two cases can be seen in Figs. 3(e) and 3(a), respectively. In Fig. 3(e) (where $\gamma_{\rm abs} = 0.10\omega_{a1}$ and $\gamma_{\rm rad} = 0.05\omega_{a1}$), the matching condition $\gamma_{\rm abs} = 2\cos^2(\varphi/2)\gamma_{\rm rad}$ is fulfilled when $\omega_{a2} = \omega_{a1}$ or $\varphi = 0$, and an emissivity spectrum with a peak value of unity, full width at half maximum (FWHM) of $0.3\omega_{a1}(= 6\gamma_{\rm rad})$, centered at $\omega = \bar{\omega} = \omega_{a1} = \omega_{a2}$ is obtained. In Fig. 3(a) (where $\gamma_{\rm abs} = 0.005\omega_{a1}$ and $\gamma_{\rm rad} = 0.05\omega_{a1}$), the matching condition $\gamma_{\rm abs} = 2\sin^2(\varphi/2)\gamma_{\rm rad}$ is fulfilled when $\omega_{a2} = \omega_{a1} \pm 0.0436\omega_{a1}$ *or* $\varphi = 2\sin^{-1}(\sqrt{\gamma_{\rm abs}/2\gamma_{\rm rad}}) = 0.144\pi$, and a narrow emissivity spectrum with a peak value of unity, FWHM of $0.03\omega_{a1}$ $(= 6\gamma_{\rm abs})$, centered at $\omega = \bar{\omega} = (1 \pm 0.0218)\omega_{a1}$ is obtained. The latter case is more interesting because FWHM of the spectrum $[6\sin^2(\varphi/2)\gamma_{\rm rad}]$ can be much narrower than the FWHM for the single-mode case with matching condition $(4\gamma_{\rm rad})$, and still shows the same high-emissivity peak near unity.

4. Subcase (ii-b): $|\omega_{a2} - \omega_{a1}| \sim 2\gamma_{\rm rad}$

When $\varphi \sim \pi/2$ or $|\omega_{a2} - \omega_{a1}| \sim 2\gamma_{\rm rad}$, the eigenmodes are nearly degenerated and have almost the same radiation decay constants of $\sim\gamma_{\rm rad}$, and the interference between $\hat{a}_+$ and $\hat{a}_-$ becomes destructive as can be seen from the phase term $(-ie^{-i\varphi}$ and $ie^{+i\varphi})$ of Eq. (36). By letting $\varphi \sim \pi/2 - \delta$ with a limit of $\delta \to 0$ and by taking into account the cancellation between the radiation from $\hat{a}_+$ and $\hat{a}_-$, we obtain the emissivity spectrum as follows:

$$\varepsilon(\omega) = 8\gamma_{\rm rad}\gamma_{\rm abs}\frac{(\bar{\omega}-\omega)^2 + \gamma_{\rm rad}^2 + \gamma_{\rm abs}^2}{\{(\bar{\omega}-\omega)^2 + (\gamma_{\rm rad}+\gamma_{\rm abs})^2\}^2}, \qquad (37)$$

where maximum emissivity of unity is obtained at $\omega = \bar{\omega}$ when $\gamma_{\rm rad} = \gamma_{\rm abs}$. In this case, the destructive interference between the two eigenmodes prevents the emissivity from exceeding unity. It is also noted that Eq. (37) is not a Lorentzian function, and indicates a more flat top shape (compared to the Lorentzian function) with FWHM of $4\sqrt{\sqrt{2}+1}\gamma_{\rm rad} \sim 6.2\gamma_{\rm rad}$ when $\gamma_{\rm rad} = \gamma_{\rm abs}$. An example of the spectrum corresponding to this case can be seen in Fig. 3(c). In Fig. 3(c) (where $\gamma_{\rm abs} = 0.05\omega_{a1}$ and $\gamma_{\rm rad} = 0.05\omega_{a1}$), $\varphi = \pi/2$ or $|\omega_{a2} - \omega_{a1}| = 2\gamma_{\rm rad}$ is obtained when $\omega_{a2} = \omega_{a1} \pm 0.1\omega_{a1}$, and the wide spectrum with peak emissivity of unity and FWHM of $0.31\omega_{a1}$ centered at $\omega = (1 \pm 0.05)\omega_{a1}$ is obtained.

B. Discussion

It is shown that two mechanisms exist when the detuning is small or the overlap of original modes is large: (ii-a) When $\omega_{a2} \sim \omega_{a1}$, a large difference of radiation and absorption decay constant matching condition for the two reconfigured eigenmodes works to prevent the emissivity from exceeding unity. (ii-b) When $|\omega_{a2} - \omega_{a1}| \sim 2\gamma_{\rm rad}$, destructive interference between the radiation from two reconfigured eigenmodes works to prevent the emissivity from exceeding unity. In the intermediate region where $0 < |\omega_{a2} - \omega_{a1}| < 2\gamma_{\rm rad}$, it is considered that both mechanisms work.

These mechanisms can be explained more intuitively and physically as follows: $\hat{a}_1$ mode is originally excited by the first thermal bath $\hat{b}_{1\mu}$, and $\hat{a}_1$ excites the radiation modes $\hat{d}_\mu$ with a phase shift of $\sim\pi/2$ as indicated by Eq. (2). As the reaction of the radiation, $\hat{a}_1$ is excited by $\hat{d}_\mu$ out of phase, which corresponds to the decay due to the radiation, indicated by the third term of Eq. (3). When the radiation modes $\hat{d}_\mu$ are common to both $\hat{a}_1$ and $\hat{a}_2$, $\hat{d}_\mu$ also excites $\hat{a}_2$ as the reaction of radiation with a phase shift of $\sim\pi/2$, which corresponds to the fourth term of the equivalent of Eq. (3) for $\hat{a}_2$. Subsequently, the excited $\hat{a}_2$ excites $\hat{d}_\mu$ out of phase as indicated by the third term of Eq. (2), which reduces the radiation $\hat{d}_\mu$. This process can be interpreted as that the radiation from the first thermal bath via $\hat{a}_1$ is partly absorbed by the second thermal bath via reaction of the radiation that works on $\hat{a}_2$. Similarly, the radiation of the second thermal bath from $\hat{a}_2$ is absorbed by the first thermal bath via reaction of the radiation that works on $\hat{a}_1$. This process reduces the amount of thermal radiation from one thermal bath when the other thermal bath exists, and this absorption becomes larger as the matching condition $\gamma_{\rm abs} = \gamma_{\rm rad}$ in the other resonant mode is more fulfilled. Therefore, when the two resonant modes are far from the matching condition and/or in large detuning condition, the thermal emission from one mode is scarcely absorbed by the other mode, and the total thermal emission is not much different from the simple sum of the emission from each mode. On the other hand, when the two modes are in nearly decay constant matching condition with small detuning, a considerable part of the radiation from each mode is absorbed by the other mode even though the original radiation is large. Therefore, the emissivity becomes much smaller than the simple sum of the emissivity from the two modes. It is considered that this mechanism also works when the two resonant modes are not identical. Although it was difficult to analyze Eq. (26) for arbitrary parameters analytically, we numerically confirmed that the emissivity represented by Eq. (26) does not exceed unity for a variety of parameters. It is also considered that the above explained mechanism generally works to prevent the emissivity from exceeding unity even when multiple overlapping resonant modes exist.

C. Enhancement of thermal emission compared with single-resonant-mode case

In a practical situation, it is important to enhance the emissivity or absorptivity in a frequency range of interest

by using a resonant mode when bare absorption by material is weak. Moreover, it is expected that the effect would be increased by using two or more resonant modes. It is physically interesting to investigate how much the light-matter interaction with respect to emissivity and absorptivity can be enhanced for a given range of concern, and how the degree of enhancement depends on the frequency range of concern. Here, we investigate the enhancement with two resonant modes and compare with the case of a resonant mode. For this purpose, we evaluated the largest attainable average emissivity and absorptivity for each frequency range of concern for a fixed absorption decay rate (which is determined by the bare absorption coefficient of the material). The average emissivity and absorptivity is the measure to indicate how strongly the emissivity and absorptivity can be enhanced compared to unity (or theoretical limit) within that frequency range of concern. Here, we assumed that $\gamma_{b1,11} = \gamma_{b2,22} (= \gamma_{\mathrm{abs}})$ because the two modes are embedded in the same material, and we evaluated the average emissivity and absorptivity in a range between $\omega_0 - \sigma/2$ and $\omega_0 + \sigma/2$, where σ and ω_0 are the frequency range of interest and its center. After searching the large parameter space, we found that largest average emissivity and absorptivity values are found when $\gamma_{d,11} = \gamma_{d,22} (\equiv \gamma_{\mathrm{rad}})$ regardless of the values of ω_{a1},ω_{a2} for every σ. Furthermore, we found that the values of ω_{a1},ω_{a2} for maximal average emissivity are symmetric about ω_0, i.e., when $\omega_0 - \omega_{a1} = \omega_{a2} - \omega_0 (\equiv \Delta\omega)$. Finally, we numerically optimized the values of γ_{rad} and $\Delta\omega$ required to maximize average emissivity and absorptivity for each σ. The obtained maximally attainable average emissivity and absorptivity are plotted in Fig. 5 as a function of σ, together with the case for a single resonant mode. It is seen in the figure that an average emissivity of larger than 0.8 can be obtained up to a frequency range of $\sim 10\gamma_{\mathrm{abs}}$ in the case of two resonant modes. This range is more than twice that for the case of a single resonant mode ($\sigma \sim 4\gamma_{\mathrm{abs}}$). Such enhancement is useful to create wide-range high-emissivity and absorptivity band in low-absorptive material using resonant modes. We believe this analysis can be extended into the cases of low-absorptive material with multiple resonant modes (>2).

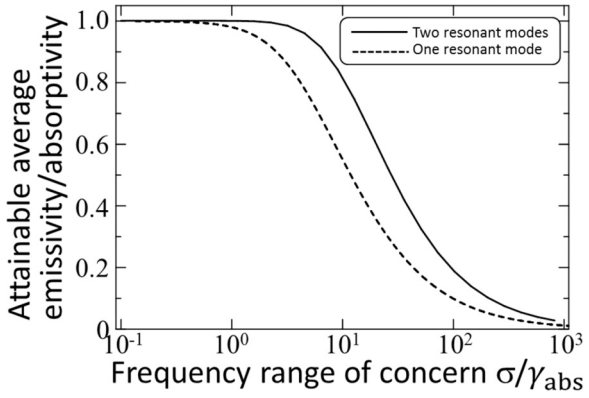

FIG. 5. Maximally attainable average emissivity and absorptivity for a frequency of interest σ (normalized by γ_{abs}) in the cases of two resonant modes (solid line) and a single resonant mode (dashed line). The frequency range where an average emissivity can be maintained larger than 0.8 is more than twice for the former compared to the latter even though the absorption rate γ_{abs} is the same.

IV. CONCLUSIONS

The thermal emission from a two-dimensional (2D) periodic structure having two guided modes has been investigated by first-principles calculations based on a model that integrates a quantum mechanical analysis of interactions involving 2D guided modes, free-space modes, and thermal baths (required to describe the radiation power), and a classical connection condition that describes coupling between the 2D guided and free-space modes (required to describe the radiation intensity). We have shown that the coupling between two guided modes via common radiation modes plays an important role in determining the emissivity spectrum when the two modes overlap with respect to frequency and solid angle in free space: the reaction of radiation modes excited by one guided mode works not only on that guided mode but also on the other guided mode so that emission from one thermal bath is absorbed by the other thermal bath and vice versa to keep the emissivity below unity. We have shown that emissivity and absorptivity spectrum much narrower or larger line width compared to the case of single resonant mode can be obtained for the case of two resonant modes by controlling the interaction between the two modes. We have also shown that the frequency range in which the emissivity and absorptivity can be enhanced >0.8 is expanded by more than a factor of 2.5 when a pair of resonant modes is utilized compared to the case single resonant mode is utilized. We believe our findings supply a physical understanding of multimode thermal emission, and will contribute to a development of methods to control the emissivity and absorptivity spectrum according to specific requirements.

ACKNOWLEDGMENTS

We thank Dr. Ardavan Oskooi and Dr. Yoshinori Tanaka for fruitful discussions. This work was supported by the Grant-in-Aid for scientific research from the Ministry of Education, Culture, Sports, Science and Technology of Japan, and by the Core Research for Evolutional Science and Technology program of the Japan Science and Technology Agency.

APPENDIX A: EXPLANATION OF THE ASSUMPTION OF INDEPENDENT THERMAL BATHS

In this Appendix, we explain why we assumed independent thermal baths for each guided modes for the analysis.

One of the model structures we supposed was a periodic array of metal cavities with different resonant wavelengths packed in a unit cell (for example, Fig. 5 of Ref. [12]). In this case, because optical fields of the metal cavities are tightly confined in each metal structure, each 2D guided mode is considered to be composed mainly from the superposition of cavities with the same resonant frequency. Therefore, the optical absorption of the different 2D guided modes takes place in different sets of metal cavities, which means that the cross terms $\gamma_{\mathrm{b1},ij}$ and $\gamma_{\mathrm{b2},ij}$ do not exist for $i \neq j$.

Another model structure we supposed was a photonic crystal slab structure with multiple guided modes (for example, Ref. [13]). In this case, the guided modes are orthogonal to each other, which means that the condition

$$\int \varepsilon(\vec{r})\vec{E}_i(\vec{r})\cdot\vec{E}_j^*(\vec{r})d\vec{r} = \delta_{i,j} \tag{A1}$$

is fulfilled, where $\vec{E}_i$ is the electric field distribution of the guided mode i and ε is the permittivity distribution of the photonic crystals. Equation (A1) means that the polarization distribution induced by mode i $[\varepsilon(\vec{r})\vec{E}_i(\vec{r})]$ is orthogonal to $\vec{E}_j(\vec{r})$ (for $i \neq j$). Here, the backreaction from the thermal bath is inseparably integrated in the polarization $\varepsilon(\vec{r})\vec{E}_i(\vec{r})$ through the imaginary part of permittivity, and therefore cannot be impinged on mode j $(\neq i)$ because $\varepsilon(\vec{r})\vec{E}_i(\vec{r})$ totally act on $\vec{E}_j(\vec{r})$ where the orthogonality condition (A1) is fulfilled. Therefore, the cross terms are considered not to exist.

APPENDIX B: EMISSION POWER SPECTRUM

In this Appendix, we explain how we derived Eq. (10). Because we have to express the power spectrum in the form rigorously comparable to the blackbody spectrum, and our analysis is based on the quantum Langevin approach where the operators have time dependence, we had to derive Eq. (10) from the Parseval's theorem as follows:

At first, we set an observation window time T, where T is a short duration within which the operators do not change largely under a rotating wave approximation but enough long to carry out Fourier transformation to obtain spectra. We evaluate the total energy of free-space modes at around time t by an average of total energy over the time from t to $t+T$ as follows:

$$U_{fs}(t) = \frac{1}{T}\int_t^{t+T}\sum_\mu \hbar\omega_\mu\langle\hat{d}_\mu^\dagger(t')\hat{d}_\mu(t')\rangle dt'. \tag{B1}$$

The power emitted to free space at around time t can be evaluated by the temporal differentiation of Eq. (B1) from the Poynting's theorem as follows:

$$P_{em}(t) = \frac{d}{dt}\left\{\frac{1}{T}\int_t^{t+T}\sum_\mu \hbar\omega_\mu\langle\hat{d}_\mu^\dagger(t')\hat{d}_\mu(t')\rangle dt'\right\}. \tag{B2}$$

Here, we define the annihilation operator of free-space modes that are Fourier transformed within the time window $[t, t+T]$ as follows:

$$\hat{d}_{\mu T}(\omega,t) = \int_t^{t+T}\hat{d}_\mu(t')e^{i\omega t'}dt'. \tag{B3}$$

It is easily confirmed that the Parseval's theorem for the time window $[t, t+T]$ can be expressed as follows:

$$\int_t^{t+T}\langle\hat{d}_\mu^\dagger(t')\hat{d}_\mu(t')\rangle dt' = \int_{-\infty}^{+\infty}\langle\hat{d}_{\mu T}^\dagger(\omega,t)\hat{d}_{\mu T}(\omega,t)\rangle d\omega. \tag{B4}$$

By using Eq. (B4), we can rewrite $P_{em}(t)$ as follows:

$$P_{em}(t) = \frac{d}{dt}\left\{\frac{1}{2\pi T}\int_{-\infty}^{+\infty}\sum_\mu \hbar\omega_\mu\langle\hat{d}_{\mu T}^\dagger(\omega,t)\hat{d}_{\mu T}(\omega,t)\rangle d\omega\right\}. \tag{B5}$$

The term $\langle\hat{d}_{\mu T}^\dagger(\omega,t)\hat{d}_{\mu T}(\omega,t)\rangle$ can be rewritten with Eq. (B3) as follows:

$$\begin{aligned}&\langle\hat{d}_{\mu T}^\dagger(\omega,t)\hat{d}_{\mu T}(\omega,t)\rangle\\ &= \left\langle\int_t^{t+T}\hat{d}_\mu^\dagger(t')e^{-i\omega t'}dt'\int_t^{t+T}\hat{d}_\mu(t'')e^{i\omega t''}dt''\right\rangle\\ &= \int_t^{t+T}\int_t^{t+T}\langle\hat{d}_\mu^\dagger(t')\hat{d}_\mu(t'')\rangle e^{-i\omega(t'-t'')}dt'dt''.\end{aligned} \tag{B6}$$

We change the integration range for t' from $[t,\ t+T]$ to $[t''-T/2,\ t''+T/2]$ using the assumption that T is a small duration within which the operators do not change largely. Under this approximation, Eq. (B6) is given by

$$\begin{aligned}&\langle\hat{d}_{\mu T}^\dagger(\omega,t)\hat{d}_{\mu T}(\omega,t)\rangle\\ &\approx \int_t^{t+T}\left\{\int_{-T/2}^{T/2}\langle\hat{d}_\mu^\dagger(t''+\tau)\hat{d}_\mu(t'')\rangle e^{-i\omega\tau}d\tau\right\}dt''.\end{aligned} \tag{B7}$$

We can also assume that the correlation function $\int_{-T/2}^{+T/2}\langle\hat{d}_\mu^\dagger(t''+\tau)\hat{d}_\mu(t'')\rangle e^{-i\omega\tau}d\tau$ does not change largely for the duration $[t, t+T]$. In this case Eq. (B7) is given as

$$\langle\hat{d}_{\mu T}^\dagger(\omega,t)\hat{d}_{\mu T}(\omega,t)\rangle \approx T\int_{-T/2}^{T/2}\langle\hat{d}_\mu^\dagger(t+\tau)\hat{d}_\mu(t)\rangle e^{-i\omega\tau}d\tau. \tag{B8}$$

We evaluate Eq. (B5) using Eq.(B8) and obtain

$$\begin{aligned}P_{em}(t) &= \frac{d}{dt}\left[\frac{1}{2\pi T}\int_{-\infty}^{+\infty}\sum_\mu \hbar\omega_\mu\left\{T\int_{-T/2}^{T/2}\langle\hat{d}_\mu^\dagger(t+\tau)\hat{d}_\mu(t)\rangle e^{-i\omega\tau}d\tau\right\}d\omega\right]\\ &= \int_{-\infty}^{+\infty}\left[\frac{1}{2\pi}\sum_\mu \hbar\omega_\mu\left\{\frac{d}{dt}\int_{-T/2}^{T/2}\langle\hat{d}_\mu^\dagger(t+\tau)\hat{d}_\mu(t)\rangle e^{-i\omega\tau}d\tau\right\}\right]d\omega.\end{aligned} \tag{B9}$$

Therefore, the Fourier spectrum of $P_{em}(t)$ can be defined as

$$P_{em}(\omega,t) = \frac{1}{2\pi}\sum_\mu \hbar\omega_\mu\left\{\frac{d}{dt}\int_{-T/2}^{T/2}\langle\hat{d}_\mu^\dagger(t+\tau)\hat{d}_\mu(t)\rangle e^{-i\omega\tau}\right\}d\tau = \frac{1}{2\pi}\frac{d}{dt}\left\{\hbar\omega\int_{-T/2}^{T/2}\sum_\mu\langle\hat{d}_\mu^\dagger(t+\tau)\hat{d}_\mu(t)\rangle e^{-i\omega\tau}d\tau\right\}, \tag{B10}$$

where

$$P_{em}(t) = \int_{-\infty}^{+\infty} P_{em}(\omega,t)d\omega \tag{B11}$$

is satisfied. Equation (B10) physically indicates that the radiation power is obtained from temporal differentiation of the Fourier spectrum of the energy in free space. Equation (B11) means the unit of $P_{em}(\omega,t)$ is energy per unit time per unit angular frequency.

Finally, we can extend the integration range of τ to $[-\infty, +\infty]$ because our window time T is assumed to be long enough to evaluate the spectrum, or T is enough larger than the correlation time for $\hat{d}_\mu(t)$. Therefore, we obtain

$$P_{em}(\omega,t) = \frac{\hbar\omega}{2\pi}\int_{-\infty}^{\infty}\sum_{\mu}\frac{d}{dt}\langle\hat{d}_\mu^\dagger(t+\tau)\hat{d}_\mu(t)\rangle e^{-i\omega\tau}d\tau, \tag{B12}$$

which is equal to Eq. (10) of the main text except that $P_{em}(\omega,t)$ is expressed as $P_{em}(\omega)$ for simplicity.

APPENDIX C: ANALYTICAL DEMONSTRATION OF $\varepsilon \leqslant 1$ FOR IDENTICAL TWO RESONANT MODES

In this Appendix, we demonstrate analytically that the emissivity does not exceed unity for the case that two resonant modes are identical except for the frequency.

At first, we obtain a more explicit form of emissivity spectra by substituting Eqs. (27)–(29) into Eq. (26) as follows:

$$\varepsilon(\omega) = \frac{4\gamma_{b2,22}\gamma_{d,22}\left\{(\omega-\omega_{a1})^2+\gamma_{b1,11}^2\right\}+4\gamma_{b1,11}\gamma_{d,11}\left\{(\omega-\omega_{a2})^2+\gamma_{b2,22}^2\right\}}{|(\lambda_+ + i\omega)(\lambda_- + i\omega)|^2}. \tag{C1}$$

Next, we introduce a function E that represents the difference between the denominator and numerator of Eq. (C1):

$$E = |(\lambda_+ + i\omega)(\lambda_- + i\omega)|^2 - 4\gamma_{b2,22}\gamma_{d,22}\left\{(\omega-\omega_{a1})^2+\gamma_{b1,11}^2\right\} - 4\gamma_{b1,11}\gamma_{d,11}\left\{(\omega-\omega_{a2})^2+\gamma_{b2,22}^2\right\}. \tag{C2}$$

This function is used to determine the condition that optimizes the peak emissivity, where an emissivity of unity corresponds to $E = 0$, and an emissivity of less than unity corresponds to $E > 0$. Equation (C2) is too complex to analyze in general cases because it is a biquadratic function. In the following, we evaluate E by limiting $\gamma_{d,11} = \gamma_{d,22} = \gamma_{\rm rad}$ and $\gamma_{b1,11} = \gamma_{b2,22} = \gamma_{\rm abs}$. There are two cases, (i) $|\omega_{a2} - \omega_{a1}| > 2\gamma_{\rm rad}$ and (ii) $|\omega_{a2} - \omega_{a1}| \leqslant 2\gamma_{\rm rad}$, that have different characteristics. We discuss them separately as follows:

1. Case (i): $|\omega_{a2} - \omega_{a1}| > 2\gamma_{\rm rad}$

The imaginary parts of $-\lambda_\pm$ are different $[\bar{\omega} \pm \sqrt{(\omega_{a2}-\omega_{a1})^2/4 - \gamma_{\rm rad}^2}]$ and the real parts of $-\lambda_\pm$ are equal $(\gamma_{\rm rad} + \gamma_{\rm abs})$. Equation (C2) can be simplified as follows:

$$E = \{(\omega-\bar{\omega})^2 + (\gamma_{\rm rad}-\gamma_{\rm abs})^2 - \delta\omega^2\}^2 + 4(\gamma_{\rm rad}-\gamma_{\rm abs})^2\delta\omega^2, \tag{C3}$$

where $\delta\omega^2 = (\omega_{a2}-\omega_{a1})^2/4 - \gamma_{\rm rad}^2$. $E = 0$ or an emissivity of unity is obtained at $\omega = \bar{\omega} \pm \delta\omega$ when $\gamma_{\rm rad} = \gamma_{\rm abs}$ is satisfied, regardless of the detuning (as long as $|\omega_{a2} - \omega_{a1}| > 2\gamma_{\rm rad}$).

2. Case (ii): $|\omega_{a2} - \omega_{a1}| \leqslant 2\gamma_{\rm rad}$

Under the condition that $|\omega_{a2} - \omega_{a1}| \leqslant 2\gamma_{\rm rad}$, the real parts of $-\lambda_\pm$ are identical $(\bar{\omega})$ and the imaginary parts of $-\lambda_\pm$ are different $[\gamma_{\rm rad} + \gamma_{\rm abs} \pm \sqrt{\gamma_{\rm rad}^2 - (\omega_{a2}-\omega_{a1})^2/4}]$. Equation (C2) can be simplified as follows:

$$E = (\omega-\bar{\omega})^4 + 2(\omega-\bar{\omega})^2\{(\gamma_{\rm rad}-\gamma_{\rm abs})^2 + \delta\gamma^2\} + \{(\gamma_{\rm rad}-\gamma_{\rm abs})^2 - \delta\gamma^2\}^2, \tag{C4}$$

where $\delta\gamma^2 = \gamma_{\rm rad}^2 - (\omega_{a2}-\omega_{a1})^2/4$. Because $\delta\gamma^2 \geqslant 0$ under the condition $|\omega_{a2} - \omega_{a1}| \leqslant 2\gamma_{\rm rad}$, Eq. (C4) is always positive or zero, which means that ε does not exceed unity. The maximal ε of unity is obtained at $\omega = \bar{\omega}$ when the last term of Eq. (C4) is zero, or when

$$|\omega_{a2} - \omega_{a1}| = 2\sqrt{\gamma_{\rm rad}^2 - (\gamma_{\rm rad}-\gamma_{\rm abs})^2}. \tag{C5}$$

Here, $\gamma_{\rm rad}^2 - (\gamma_{\rm rad} - \gamma_{\rm abs})^2$ must be positive or zero to satisfy Eq. (C5), which requires $2\gamma_{\rm rad} \geqslant \gamma_{\rm abs}$.

[1] J. F. Waymouth, J. Light Visual Environ. **13**, 51 (1989).
[2] S. Maruyama, T. Kashiwa, H. Yugami, and M. Esashi, Appl. Phys. Lett. **79**, 1393 (2001).
[3] M. U. Pralle, N. Moelders, M. P. McNeal, I. Puscasu, A. C. Greenwald, J. T. Daly, E. A. Johnson, T. George, D. S. Choi, I. El-Kady, and R. Biswas, Appl. Phys. Lett. **81**, 4685 (2002).
[4] F. Kusunoki, J. Takahara, and T. Kobayashi, Electron. Lett. **39**, 23 (2003).
[5] S. Y. Lin, J. Moreno, and J. G. Fleming, Appl. Phys. Lett. **83**, 380 (2003).

[6] C. Luo, A. Narayanaswamy, G. Chen, and J. D. Joannopoulos, Phys. Rev. Lett. **93**, 213905 (2004).
[7] J. T. K. Wan and C. T. Chan, Appl. Phys. Lett. **89**, 041915 (2006).
[8] D. L. C. Chan, M. Soljacic, and J. D. Joannopoulos, Opt. Express **14**, 8785 (2006).
[9] D. L. C. Chan, I. Celanovic, J. D. Joannopoulos, and M. Soljačić, Phys. Rev. A **74**, 064901 (2006).
[10] K. Ikeda, H. T. Miyazaki, T. Kasaya, K. Yamamoto, Y. Inoue, K. Fujimura, T. Kanakugi, M. Okada, K. Hatade, and S. Kitagawa, Appl. Phys. Lett. **92**, 021117 (2008).
[11] T. Asano, K. Mochizuki, M. Yamaguchi, M. Chaminda, and S. Noda, Opt. Express **17**, 19190 (2009).
[12] X. Liu, T. Tyler, T. Starr, A. F. Starr, N. M. Jokerst, and W. J. Padilla, Phys. Rev. Lett. **107**, 045901 (2011).
[13] M. De Zoysa, T. Asano, K. Mochizuki, A. Oskooi, T. Inoue, and S. Noda, Nat. Photonics **6**, 535 (2012).
[14] T. Inoue, T. Asano, M. De Zoysa, A. Oskooi, and S. Noda, J. Opt. Soc. Am. B **30**, 165 (2013).
[15] T. Inoue, M. De Zoysa, T. Asano, and S. Noda, Appl. Phys. Lett. **102**, 191110 (2013).
[16] R. M. Swanson, Proc. IEEE **67**, 446 (1979).
[17] P. Berme, M. Ghebrebrhan, W. Chan, Y. X. Yeng, M. Araghchini, R. Hamam, C. H. Marton, K. F. Jensen, M. Soljacic, J. D. Joannopoulos, S. G. Johnson, and I. Celanovic, Opt. Express **18**, A314 (2010).
[18] Z. Yu, A. Raman, and S. Fan, Proc. Natl. Acad. Sci. USA **107**, 17491 (2010).
[19] H. Shigeta, M. Fujita, Y. Tanaka, A. Oskooi, H. Ogawa, Y. Tsuda, and S. Noda, Appl. Phys. Lett. **101**, 161103 (2012).
[20] A. Oskooi, P. A. Favuzzi, Y. Tanaka, H. Shigeta, Y. Kawakami, and S. Noda, Appl. Phys. Lett. **100**, 181110 (2012).
[21] Y. Tanaka, Y. Kawamoto, M. Fujita, and S. Noda, Opt. Express **21**, 20111 (2013).